Assessment of Differential Carrier Phase Measurements from Orbcomm LEO Satellite Signals for Opportunistic Navigation

Joe Khalife and Zaher M. Kassas
University of California, Irvine

BIOGRAPHIES

Joe J. Khalife is a Ph.D. student at the University of California, Irvine and member of the Autonomous Systems Perception, Intelligence, and Navigation (ASPIN) Laboratory. He received a B.E. in electrical engineering and an M.S. in computer engineering from the Lebanese American University (LAU). From 2012 to 2015, he was a research assistant at LAU. His research interests include opportunistic navigation, autonomous vehicles, and software-defined radio.

Zaher (Zak) M. Kassas is an assistant professor at the University of California, Irvine and director of the ASPIN Laboratory. He received a B.E. in Electrical Engineering from the Lebanese American University, an M.S. in Electrical and Computer Engineering from The Ohio State University, and an M.S.E. in Aerospace Engineering and a Ph.D. in Electrical and Computer Engineering from The University of Texas at Austin. In 2018, he received the National Science Foundation (NSF) Faculty Early Career Development Program (CAREER) award, and in 2019, he received the Office of Naval Research (ONR) Young Investigator Program (YIP) award. His research interests include cyber-physical systems, estimation theory, navigation systems, autonomous vehicles, and intelligent transportation systems.

ABSTRACT

A framework for positioning with carrier phase differential (CD) - low Earth orbit (LEO) (CD-LEO) measurements is developed. This framework utilizes a base and a rover and enables navigation with the Orbcomm LEO constellation without requiring prior knowledge of the rover's position. The effect of ionospheric and tropospheric delays on the carrier phase and CD-LEO measurements are discussed. The residual ionospheric and tropospheric delays are studied as a function of the baseline. Moreover, the position dilution of precision (PDOP) is studied for the Orbcomm constellation, and it is found that a less than unity PDOP may be achieved for 8-minute wait times. Experimental results show a receiver positioning itself exclusively with CD-LEO measurements from two Orbcomm satellites with a position error of 11.93 m.

I. INTRODUCTION

The promise of broadband low Earth orbit (LEO) satellite signals as a desirable navigation and timing source has been demonstrated in the past decade [1–6]. While some of these approaches call for tailoring the broadband protocol to support navigation capabilities [3, 7], others exploit existing broadband LEO constellations for navigation in an opportunistic fashion [2, 4, 8–10]. The former approaches allow for simpler receiver architectures and navigation algorithms. However, they require significant changes to existing infrastructure, the cost of which private companies (e.g., OneWeb, SpaceX, and Boeing), which are planning to aggregately launch thousands of broadband Internet satellites into LEO, may not be willing to pay. Moreover, if these companies agree to that additional cost, there will be no guarantees that they would not charge for "extra navigation services." In this case, exploiting broadband LEO satellite signals opportunistically for navigation becomes the more attractive approach. This paper assesses opportunistic navigation with differential carrier phase measurements from broadband LEO satellite signals.

Opportunistic navigation, or navigation with signals of opportunity (SOPs), has been recently considered as a reliable alternative paradigm to GNSS navigation [11]. Besides broadband LEO satellite signals, other SOPs include AM/FM radio [12,13], WiFi [14,15], and cellular [16–20], with the latter showing the promise of a submeter-accurate navigation solution for unmanned aerial vehicles when carrier phase measurements from cellular signals are used

Preprint of the 2019 ION GNSS+ Conference
Miami, FL, September 16–20, 2019

[21, 22]. LEO satellites possess desirable attributes for positioning: (i) they are around twenty times closer to the Earth compared to GNSS satellites, which reside in medium Earth orbit (MEO), making their received signal power between 24 to 34 dBs higher than GNSS signals; (ii) they will become abundant as thousands of broadband Internet satellites are expected to be deployed into LEO [3]; and (iii) each broadband provider will deploy broadband Internet satellites into unique constellations, transmitting at different frequency bands, making LEO satellite signals diverse in frequency and direction [23]. Moreover, the Keplerian elements parameterizing the orbits of these LEO satellites are made publicly available by the North American Aerospace Defense Command (NORAD) and are updated daily in the two-line element (TLE) files. Using TLEs and orbit determination algorithms (e.g., SGP 4), the positions and velocities of these satellites can be known, albeit not precisely. In addition, some of these broadband LEO satellites, such as Orbcomm satellites, are equipped with GPS receivers and broadcast their GPS solution to the terrestrial receivers.

This paper considers the problem of positioning exclusively with LEO satellite signals in the inevitable case where GNSS signals become unavailable or unreliable (e.g., in jammed or spoofed environments). To this end, there are several challenges to overcome, mainly the absence of: (i) publicly available receivers that can extract navigation observables from LEO satellite signals, (ii) source of error characterization for designing LEO satellite navigation frameworks, and (iii) performance analyses tools to evaluate these frameworks. The first challenge has been mainly addressed for Orbcomm satellite signals [9]. This paper makes three contributions that address the second and third challenges mainly for the Orbcomm constellation. First, a carrier phase differential (CD)-LEO navigation framework is developed for real broadband LEO satellite signals. Second, the estimability of the receiver's position is studied and a rule of thumb for setting the size of the batch estimator from the number of available satellites to meet performance requirements is developed. Third, the effect of residual ionospheric and tropospheric delays on the double-difference carrier phase measurements is studied, and the tradeoff between coverage and accuracy is discussed.

The high precision of carrier phase measurements enables very precise navigation, as demonstrated in GPS and cellular SOPs [21]. However, this precision comes at the cost of added ambiguities that need to be estimated. Consider a receiver on-board a "rover" on Earth making carrier phase measurements to broadband LEO satellites and a "base" station in the vicinity of the rover making carrier phase measurements to the same LEO satellites. One can form the double-difference carrier phase measurements from the base and rover measurements and solve for the rover's position as well as for the resulting ambiguities. One important measure of the estimability (or degree of observability) of the rover's position is the position dilution of precision (PDOP). If no position prior is available, the rover cannot perform real-time positioning and must wait until there is enough change in satellite geometry and solve a batch least-squares to estimate its position and the carrier phase ambiguities. Significant change in geometry is required particularly for current broadband LEO constellations where the average number of visible satellites is less than three. The wait time depends on several variables but is mainly determined by the desired PDOP and the number of available satellites. Fortunately, due to the desirable properties of LEO, this wait time is much less than in the case of GPS.

Aside from carrier phase ambiguities, another major source of error that has to be considered in the CD-LEO framework is the ionospheric and tropospheric delays, since most broadband LEO constellations reside above the ionosphere. The magnitude of the ionospheric delay is (i) inversely proportional to the square of the carrier frequency and (ii) proportional to the obliquity factor, which is related to the elevation angle. This relationship becomes crucial for the proposed framework since: (i) Orbcomm satellite signals, which are transmitted in the very high frequency (VHF) band, will experience significantly larger ionospheric delays than GPS L1 signals, and (ii) due to Orbcomm satellites residing in LEO orbits, the obliquity factor changes significantly between different points on Earth, which introduces large ionospheric and tropospheric delay residuals. Although the double-difference carrier phase measurements will cancel out most of the errors due to ionospheric delays, there will still be significant errors if the base and rover are "too" far apart. For relatively long baselines, these errors become too large to be ignored if an accurate navigation solution is desired. Subsequently, there exists a tradeoff between coverage and accuracy, in that one would like to minimize the number of differential base stations needed while guaranteeing a certain accuracy.

The proposed CD-LEO framework is demonstrated experimentally using proprietary Orbcomm software-defined receivers (SDRs) developed at the Autonomous Systems Perception, Intelligence, and Navigation (ASPIN) laboratory. The SDRs are implemented on a host computer with a universal software radio peripheral (USRP) serving as an RF

front-end. The GPS-based LEO satellite positions are decoded from the transmitted Orbcomm satellite messages. Experimental results are presented showing a receiver localizing itself with real Orbcomm satellite signals using the proposed CD-LEO framework with a position error of 11.93 m.

The rest of the paper is organized as follows. Section II describes the carrier phase measurement model and the ionospheric and tropospheric delay models. Section III discusses the CD-LEO framework. Section IV characterizes the performance of the proposed CD-LEO framework by studying the PDOP and the residual ionospheric and tropospheric delays for the Orbcomm constellation. Section V shows experimental results demonstrating a receiver positioning with the proposed CD-LEO framework. Section VI gives concluding remarks.

II. MODEL DESCRIPTION

This section describes the carrier phase measurement model and the ionospheric and tropospheric delay models used in the rest of the paper.

A. LEO CARRIER PHASE OBSERVATION MODEL

In this paper, availability of Doppler frequency measurements of Orbcomm LEO space vehicle (SV) signals from the specialized navigation receiver in [9] is assumed. The continuous-time carrier phase observable can be obtained by integrating the Doppler measurement over time [24]. The carrier phase (expressed in cycles) made by the i-th receiver on the l-th LEO SV is given by

$$\phi_l^{(i)}(t) = \phi_l^{(i)}(t_0) + \int_{t_0}^{t} f_{D_l}^{(i)}(\tau)d\tau, \quad l = 1, \ldots, L, \tag{1}$$

where $f_{D_l}^{(i)}$ is the Doppler measurement made by the i-th receiver on the l-th LEO SV, $\phi_l^{(i)}(t_0)$ is the initial carrier phase, and L is the total number of visible LEO SVs. In (1), i denotes either the base B or the rover R. Assuming a constant Doppler during a subaccumulation period T, (1) can be discretized to yield

$$\phi_l^{(i)}(t_k) = \phi_l^{(i)}(t_0) + \sum_{n=0}^{k-1} f_{D_l}^{(i)}(t_n)T, \tag{2}$$

where $t_k \triangleq t_0 + kT$. In what follows, the time argument t_k will be replaced by k for simplicity of notation. Note that the receiver will make noisy carrier phase measurements. Adding measurement noise and the ionospheric and tropospheric delays to (2) and expressing the carrier phase observable in meters yields

$$z_l^{(i)}(k) = \lambda_l \phi_l^{(i)}(0) + \lambda_l T \sum_{n=0}^{k-1} f_{D_l}^{(i)}(n) + v_l^{(i)}(k), \tag{3}$$

where λ_l is the wavelength of the carrier signal transmitted by the l-th LEO SV and $v_l^{(i)}(k)$ is the measurement noise, which is modeled as a discrete-time zero-mean white Gaussian sequence with variance $\left[\sigma_l^{(i)}(k)\right]^2$, which can be shown to be given by [9]

$$\left[\sigma_l^{(i)}(k)\right]^2 = \frac{2\lambda_l^2 B_{i,\mathrm{PLL}} T}{\left(\mathrm{SNR}_l^{(i)}(k)\right)^3}\left[\frac{8}{9\left(\mathrm{SNR}_l^{(i)}(k)\right)^4} + \frac{20}{3\left(\mathrm{SNR}_l^{(i)}(k)\right)^3} + \frac{10}{3\left(\mathrm{SNR}_l^{(i)}(k)\right)^2} - \frac{8}{3\left(\mathrm{SNR}_l^{(i)}(k)\right)} + 2\right],$$

where $B_{i,\mathrm{PLL}}$ is the i-th receiver's phase lock loop (PLL) noise equivalent bandwidth and $\mathrm{SNR}_l^{(i)}(k)$ is the l-th LEO SV signal-to-noise ratio at time-step k measured by the i-th receiver. Note that since LEO satellite orbits are above the ionosphere, their signals will suffer from ionospheric and tropospheric delays. Let $\delta t_{\mathrm{iono,l}}^{(i)}(k)$ and $\delta t_{\mathrm{trop,l}}^{(i)}(k)$ denote the ionospheric and tropospheric delays from the l-th LEO SV to the i-th receiver at time-step k, respectively. Subsequently, the carrier phase in (3) can be parameterized in terms of the receiver and LEO SV states as

$$z_l^{(i)}(k) = \left\|\boldsymbol{r}_{r_i} - \boldsymbol{r}_{\mathrm{leo}_l}(k)\right\|_2 + c\left[\delta t_{r_i}(k) - \delta t_{\mathrm{leo}_l}(k)\right] + \lambda_l N_l^{(i)} + c\delta t_{\mathrm{trop},l}^{(i)}(k) + c\delta t_{\mathrm{iono},l}^{(i)}(k) + v_l^{(i)}(k), \tag{4}$$

where $\boldsymbol{r}_{r_i} \triangleq [x_{r_i}, y_{r_i}, z_{r_i}]^\mathsf{T}$ is the i-th receiver's position vector; $\boldsymbol{r}_{\text{leo}_l} \triangleq [x_{\text{leo}_l}, y_{\text{leo}_l}, z_{\text{leo}_l}]^\mathsf{T}$ is the l-th LEO SV position vector; c is the speed of light; δt_{r_i} and δt_{leo_l} are the i-th receiver's and l-th LEO SV clock biases, respectively; and $N_l^{(i)}$ is the carrier phase ambiguity.

B. Ionospheric and Tropospheric Delays

For radio frequency (RF) signals transmitted at a carrier exceeding 1 MHz, the excess phase delay due to propagation in the ionosphere can be approximated by

$$\delta t_{\text{iono},l}^{(i)}(k) = -\frac{40.3 \times 10^{16} \times \alpha_{\text{iono}}\left(\theta_l^{(i)}(k)\right) \times \text{TECV}^{(i)}(k)}{c f_{c,l}^2}, \tag{5}$$

where $\theta_l^{(i)}(k)$ is the elevation angle of the l-th LEO SV with respect to the i-th receiver at time-step k; $f_{c,l}$ is the l-th LEO SV's carrier frequency; $\alpha_{\text{iono}}(\cdot)$ is the obliquity factor for a given elevation angle; and $\text{TECV}^{(i)}(k)$ is the total electron count at the i-th receiver's zenith (i.e., when the elevation angle is $\pi/2$) [24]. Note that $\text{TECV}^{(i)}(k)$ in (5) is expressed in TEC Units (TECU) and is assumed to be constant during satellite visibility. Note that a map for TECV for the i-th receiver's location at different times can be accessed online [25]. The obliquity factor is given by

$$\alpha_{\text{iono}}(u) = \left[1 - \left(\frac{R_E \cos u}{R_E + h_I}\right)^2\right]^{-\frac{1}{2}},$$

where R_E is the average radius of the Earth and h_I is the mean ionospheric height, which is taken to be 350 km.

Tropospheric delays can be modeled as the sum of two terms: the first due to dry gazes in the atmosphere and the second due to water vapor in the atmosphere. The corresponding delays are called dry and wet delays, respectively, and the total tropospheric delay is modeled as

$$\delta t_{\text{trop},l}^{(i)}(k) = \delta t_{z,w}^{(i)} \alpha_{\text{trop},w}\left(\theta_l^{(i)}(k)\right) + \delta t_{z,d}^{(i)} \alpha_{\text{trop},d}\left(\theta_l^{(i)}(k)\right), \tag{6}$$

where $\delta t_{z,w}^{(i)}$ and $\delta t_{d,w}^{(i)}$ are the wet and dry delays at the i-th receiver's zenith, respectively, and $\alpha_{\text{trop},w}(\cdot)$ and $\alpha_{\text{trop},d}(\cdot)$ are the wet and dry tropospheric obliquity factors, respectively. The obliquity factors may be approximated by

$$\alpha_{\text{trop},w}(u) = \frac{1}{\sin u + \frac{0.00035}{\tan u + 0.017}},$$
$$\alpha_{\text{trop},d}(u) = \frac{1}{\sin u + \frac{0.00143}{\tan u + 0.0445}}.$$

Using the Hopfield model, the wet and dry delays may be approximated with

$$\delta t_{z,w}^{(i)} = 0.373 \frac{e_0^{(i)}}{c\left(T_0^{(i)}\right)^2} \frac{h_w}{5}, \quad \delta t_{z,d}^{(i)} = 77.6 \times 10^{-6} \frac{P_0^{(i)}}{c T_0^{(i)}} \frac{h_d}{5},$$

where $T_0^{(i)}$ is the temperature (kelvin), $P_0^{(i)}$ is the total pressure and $e_0^{(i)}$ is the partial pressure due to water vapor (both in millibars), $h_w = 12$ km, and $h_d \approx 43$ km [24].

Fig. 1 shows the sum of simulated ionospheric and tropospheric delays for 5 Orbcomm LEO SVs transmitting in the VHF band and 5 GPS SVs at L1 frequency over a period of 4 hours. It can be seen that the ionospheric delays for Orbcomm SVs are orders of magnitude higher than those of GPS SVs due to the difference in transmit frequency.

III. NAVIGATION WITH LEO CARRIER PHASE DIFFERENTIAL MEASUREMENTS

In this section, a framework for CD-LEO navigation is developed.

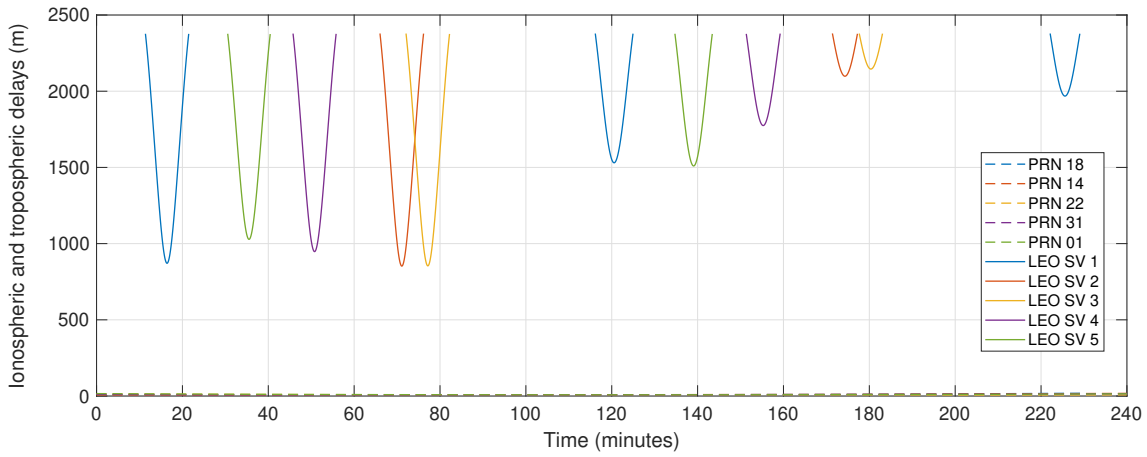

Fig. 1. Simulated delays in meters due to ionosphere and troposphere propagation for 5 Orbcomm LEO SVs and 5 GPS SVs.

A. CD-LEO FRAMEWORK

The framework consists of a rover and a base receiver in an environment comprising L visible LEO SVs. The base receiver (B), is assumed to have knowledge of its own position state, e.g., a stationary receiver deployed at a surveyed location or a high-flying unmanned aerial vehicle (UAV) with access to GNSS or one equipped with a sophisticated sensor suite. The rover (R) does not have knowledge of its position. The base communicates its own position and carrier phase observables with the rover. The LEO SVs' positions are known through the TLE files and orbit determination software, or by decoding the transmitted ephemeris, if any. Fig. 2 illustrates the base/rover CD-LEO framework.

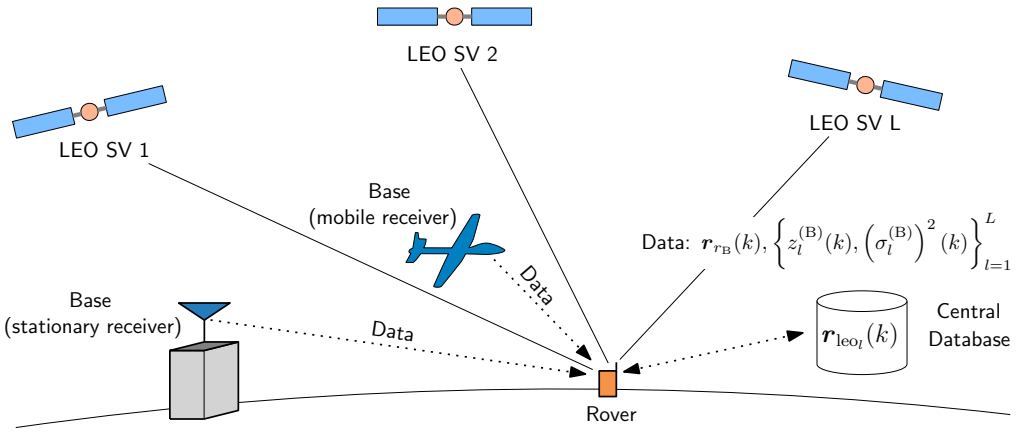

Fig. 2. Base/rover CD-LEO framework.

In what follows, the objective is to estimate the rover's position, which will be achieved by double-differencing the measurements (4). Without loss of generality, let the measurements to the first LEO SV be taken as references to form the single difference

$$z_{l,1}^{(i)}(k) \triangleq z_l^{(i)}(k) - z_1^{(i)}(k).$$

Subsequently, define the double difference between R and B as

$$\begin{aligned} z_{l,1}^{(\mathrm{R,B})}(k) &\triangleq z_{l,1}^{(\mathrm{R})}(k) - z_{l,1}^{(\mathrm{B})}(k) + \|\boldsymbol{r}_{r_\mathrm{B}} - \boldsymbol{r}_{\mathrm{leo}_l}(k)\|_2 - \|\boldsymbol{r}_{r_\mathrm{B}} - \boldsymbol{r}_{\mathrm{leo}_1}(k)\|_2 \\ &\triangleq h_{l,1}^{(\mathrm{R})}(k) + A_{l,1}^{(\mathrm{R,B})} + c\Delta_{\mathrm{iono}_{l,1}}^{(\mathrm{R,B})}(k) + c\Delta_{\mathrm{trop}_{l,1}}^{(\mathrm{R,B})}(k) + v_{l,1}^{(\mathrm{R,B})}(k), \end{aligned} \tag{7}$$

where $l = 1, \ldots, L$, and

$$
\begin{aligned}
h_{l,1}{}^{(\mathrm{R})}(k) &\triangleq \|\boldsymbol{r}_{r_\mathrm{R}} - \boldsymbol{r}_{\mathrm{leo}_l}(k)\|_2 - \|\boldsymbol{r}_{r_\mathrm{R}} - \boldsymbol{r}_{\mathrm{leo}_1}(k)\|_2 \\
A_{l,1}^{(\mathrm{R,B})} &\triangleq \lambda_l N_l^{(\mathrm{R})} - \lambda_l N_l^{(\mathrm{B})} - \lambda_1 N_1^{(\mathrm{R})} + \lambda_1 N_1^{(\mathrm{B})} \\
\Delta_{\mathrm{iono}_{l,1}}^{(\mathrm{R,B})}(k) &\triangleq \delta t_{\mathrm{iono},l}^{(\mathrm{R})}(k) - \delta t_{\mathrm{iono},l}^{(\mathrm{B})}(k) - \delta t_{\mathrm{iono},1}^{(\mathrm{R})}(k) + \delta t_{\mathrm{iono},1}^{(\mathrm{B})}(k) \\
\Delta_{\mathrm{trop}_{l,1}}^{(\mathrm{R,B})}(k) &\triangleq \delta t_{\mathrm{trop},l}^{(\mathrm{R})}(k) - \delta t_{\mathrm{trop},l}^{(\mathrm{B})}(k) - \delta t_{\mathrm{trop},1}^{(\mathrm{R})}(k) + \delta t_{\mathrm{trop},1}^{(\mathrm{B})}(k) \\
v_{l,1}^{(\mathrm{R,B})}(k) &\triangleq v_l^{(\mathrm{R})}(k) - v_l^{(\mathrm{B})}(k) - v_1^{(\mathrm{R})}(k) + v_1^{(\mathrm{B})}(k).
\end{aligned}
$$

Note that since λ_l is not necessarily equal to λ_1, then $A_{l,1}^{(\mathrm{R,B})}$ cannot necessarily be expressed as $\lambda_l M$, where M is an integer. Therefore, $A_{l,1}^{(\mathrm{R,B})}$ is hereafter considered as a real constant parameter. Moreover, this paper assumes complete knowledge of the base's position and accounts for it in the measurement defined in (7). Thus, it is expected that a mobile base and a static base will yield the same positioning performance. Define the vector of measurements

$$
\boldsymbol{z}(k) \triangleq \boldsymbol{h}_\mathrm{R}(k) + \boldsymbol{A} + c\boldsymbol{\Delta}_\mathrm{iono}(k) + c\boldsymbol{\Delta}_\mathrm{trop}(k) + \boldsymbol{v}(k),
$$

where

$$
\begin{aligned}
\boldsymbol{z}(k) &\triangleq \left[z_{2,1}^{(\mathrm{R,B})}(k), \ldots, z_{L,1}^{(\mathrm{R,B})}(k)\right]^\mathsf{T} \\
\boldsymbol{h}_\mathrm{R}(k) &\triangleq \left[h_{2,1}^{(\mathrm{R})}(k), \ldots, h_{L,1}^{(\mathrm{R})}(k)\right]^\mathsf{T} \\
\boldsymbol{A} &\triangleq \left[A_{2,1}^{(\mathrm{R,B})}, \ldots, A_{L,1}^{(\mathrm{R,B})}\right]^\mathsf{T} \\
\boldsymbol{\Delta}_\mathrm{iono}(k) &\triangleq \left[\Delta_{\mathrm{iono}_{2,1}}^{(\mathrm{R,B})}(k), \ldots, \Delta_{\mathrm{iono}_{L,1}}^{(\mathrm{R,B})}(k)\right]^\mathsf{T} \\
\boldsymbol{\Delta}_\mathrm{trop}(k) &\triangleq \left[\Delta_{\mathrm{trop}_{2,1}}^{(\mathrm{R,B})}(k), \ldots, \Delta_{\mathrm{trop}_{L,1}}^{(\mathrm{R,B})}(k)\right]^\mathsf{T} \\
\boldsymbol{v}(k) &\triangleq \left[v_{2,1}^{(\mathrm{R,B})}(k), \ldots, v_{L,1}^{(\mathrm{R,B})}(k)\right]^\mathsf{T},
\end{aligned}
$$

where $\boldsymbol{v}(k)$ has a covariance $\mathbf{R}_{\mathrm{R,B}}(k)$ which can be readily shown to be

$$
\mathbf{R}_{\mathrm{R,B}}(k) = \mathbf{R}^{(1)}(k) + \left\{\left[\sigma_1^{(\mathrm{R})}(k)\right]^2 + \left[\sigma_1^{(\mathrm{B})}(k)\right]^2\right\}\boldsymbol{\Xi},
$$

where

$$
\mathbf{R}^{(1)}(k) \triangleq \mathrm{diag}\left\{\left[\sigma_2^{(\mathrm{R})}(k)\right]^2 + \left[\sigma_2^{(\mathrm{B})}(k)\right]^2, \ldots, \left[\sigma_L^{(\mathrm{R})}(k)\right]^2 + \left[\sigma_L^{(\mathrm{B})}(k)\right]^2\right\}
$$

and $\boldsymbol{\Xi}$ is a matrix of ones.

B. BATCH SOLUTION

The vector $\boldsymbol{A}$ is unknown and has to be solved for along with the rover's position. Using only one set of carrier phase measurement with no *a priori* knowledge on the rover position results in an underdetermined system: $(L+2)$ unknowns with only $(L-1)$ measurements. Therefore, when no *a priori* information on the position of the rover is known, the rover could remain stationary for a period of time such that enough variation in satellite geometry is observed. Subsequently, the rover uses measurements collected at different times in a batch estimator, resulting in an overdetermined system [24]. Denote K the number of time-steps in which carrier phase measurements are collected to be processed in a batch, then the total number of measurements will be $K \times (L-1)$ while the total number of unknowns will remain $L+2$. Note that for $L \geq 2$, the resulting system is overdetermined for $K \geq 4$.

Define the collection of measurements from time-step 0 to $K-1$ as

$$
\mathbf{z}^K \triangleq \left[\boldsymbol{z}^\mathsf{T}(0), \ldots, \boldsymbol{z}^\mathsf{T}(K-1)\right]^\mathsf{T},
$$

which can be expressed as

$$\mathbf{z}^K = \mathbf{h}^K\left[\boldsymbol{r}_{r_\mathrm{R}}\right] + \bar{\mathbf{I}}^K \boldsymbol{A} + c\boldsymbol{\Delta}^K_{\mathrm{iono}} + c\boldsymbol{\Delta}^K_{\mathrm{trop}} + \mathbf{v}^K, \tag{8}$$

$$\mathbf{h}^K\left[\boldsymbol{r}_{r_\mathrm{R}}\right] \triangleq \begin{bmatrix} \boldsymbol{h}_\mathrm{R}(0) \\ \vdots \\ \boldsymbol{h}_\mathrm{R}(K-1) \end{bmatrix}, \quad \bar{\mathbf{I}}^K \triangleq \begin{bmatrix} \mathbf{I}_{(L-1)\times(L-1)} \\ \vdots \\ \mathbf{I}_{(L-1)\times(L-1)} \end{bmatrix},$$

$$\boldsymbol{\Delta}^K_{\mathrm{iono}} \triangleq \begin{bmatrix} \boldsymbol{\Delta}_{\mathrm{iono}}(0) \\ \vdots \\ \boldsymbol{\Delta}_{\mathrm{iono}}(K-1) \end{bmatrix}, \quad \boldsymbol{\Delta}^K_{\mathrm{trop}} \triangleq \begin{bmatrix} \boldsymbol{\Delta}_{\mathrm{trop}}(0) \\ \vdots \\ \boldsymbol{\Delta}_{\mathrm{trop}}(K-1) \end{bmatrix}, \quad \mathbf{v}^K \triangleq \begin{bmatrix} \boldsymbol{v}(0) \\ \vdots \\ \boldsymbol{v}(K-1) \end{bmatrix},$$

where $\mathbf{v}^K$ is the overall measurement noise with covariance $\mathbf{R}^K \triangleq \mathrm{diag}\left[\mathbf{R}_{\mathrm{R,B}}(0), \ldots, \mathbf{R}_{\mathrm{R,B}}(K-1)\right]$. Note that the measurements in (8) contain the ionospheric and tropospheric delays, which can be estimated according to Subsection II-B. Let $\hat{\boldsymbol{\Delta}}^K_{\mathrm{iono}}$ and $\hat{\boldsymbol{\Delta}}^K_{\mathrm{trop}}$ denote the estimates of $\boldsymbol{\Delta}^K_{\mathrm{iono}}$ and $\boldsymbol{\Delta}^K_{\mathrm{trop}}$, respectively, with the associated estimation errors

$$\tilde{\boldsymbol{\Delta}}^K_{\mathrm{iono}} \triangleq \boldsymbol{\Delta}^K_{\mathrm{iono}} - \hat{\boldsymbol{\Delta}}^K_{\mathrm{iono}}, \quad \tilde{\boldsymbol{\Delta}}^K_{\mathrm{trop}} \triangleq \boldsymbol{\Delta}^K_{\mathrm{trop}} - \hat{\boldsymbol{\Delta}}^K_{\mathrm{trop}}.$$

Subsequently, define the ionospheric delay- and tropospheric delay-free measurements

$$\begin{aligned} \bar{\mathbf{z}}^K &\triangleq \mathbf{z}^K - c\left(\hat{\boldsymbol{\Delta}}^K_{\mathrm{iono}} + \hat{\boldsymbol{\Delta}}^K_{\mathrm{trop}}\right), \\ &= \mathbf{h}^K\left[\boldsymbol{r}_{r_\mathrm{R}}\right] + \bar{\mathbf{I}}^K \boldsymbol{A} + \bar{\mathbf{v}}^K, \end{aligned} \tag{9}$$

where $\bar{\mathbf{v}}^K = \mathbf{v}^K + c\tilde{\boldsymbol{\Delta}}^K_{\mathrm{iono}} + c\tilde{\boldsymbol{\Delta}}^K_{\mathrm{trop}}$ is the overall measurement noise with the assumed covariance

$$\bar{\mathbf{R}}^K = \mathbf{R}^K + \sigma^2_{\mathrm{iono,trop}}\mathbf{I}_{K(L-1)\times K(L-1)},$$

and $\sigma^2_{\mathrm{iono,trop}}$ is a tuning parameter determined empirically. A weighted nonlinear least-squares (WNLS) estimator with weighting matrix $\left(\bar{\mathbf{R}}^K\right)^{-1}$ is used to estimate $\boldsymbol{r}_{r_\mathrm{R}}$ along with $\boldsymbol{A}$. Let $\mathbf{H}$ denote the measurement Jacobian matrix, which is given by

$$\mathbf{H} = \left[\frac{\partial}{\partial \boldsymbol{r}_{r_\mathrm{R}}}\mathbf{h}^K\left[\boldsymbol{r}_{r_\mathrm{R}}\right] \quad \bar{\mathbf{I}}^K\right].$$

IV. PERFORMANCE CHARACTERIZATION

This section characterizes the performance of the proposed CD-LEO framework by studying: (i) the PDOP and (ii) the residual ionospheric and tropospheric delays for the Orbcomm constellation.

A. PDOP Characterization

One important measure of the estimability (or degree of observability) of the rover's position is the position dilution of precision (PDOP), given by

$$\mathrm{PDOP} = \mathrm{trace}\left[\mathbf{P}_{\boldsymbol{r}}\right],$$

where $\mathbf{P}_{\boldsymbol{r}}$ corresponds to the top 3×3 block of the matrix $\left(\mathbf{H}^\mathsf{T}\mathbf{H}\right)^{-1}$. In the sequel, it is assumed that the rover is equipped with an altimeter; hence it knows its altitude. Subsequently, only the rover's horizontal position is estimated. As a result, the PDOP now corresponds to the horizontal dilution of precision (HDOP). Figure 3 shows $\ln\left[\mathrm{PDOP}\right]$ for 2 and 3 Orbcomm satellites at two positions on Earth (Seattle, WA, USA, and Quito, Ecuador) as a function of time.

Next, heat maps of $\ln\left[\mathrm{PDOP}\right]$ are generated for the entire globe starting midnight on June 27, 2019, UTC time. Four maps are generated, each 30 minutes apart, showing the PDOP obtained after an 8-minute wait time, and are shown in Fig. 4.

The heat map combining the 4 heat maps is shown in Fig. 5.

It can be seen from Fig. 4(a)–(d) and Fig. 5 that a less than unity PDOP can be achieved for an 8-minute wait time, implying submeter-accurate positioning with Orbcomm satellites.

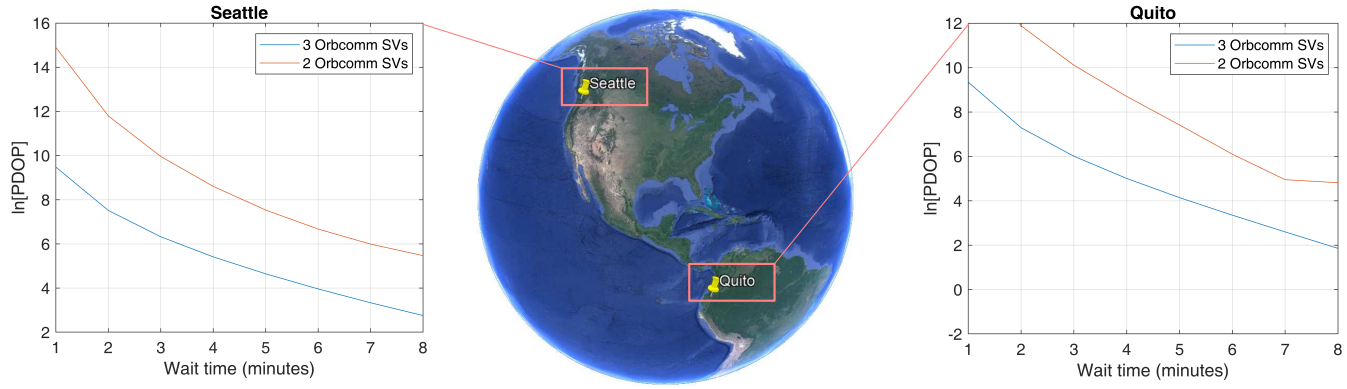

Fig. 3. Logarithm of the PDOP as a function of time at two positions on Earth (Seattle, WA, USA, and Quito, Ecuador) for 2 and 3 Orbcomm satellites. Map data: Google Earth.

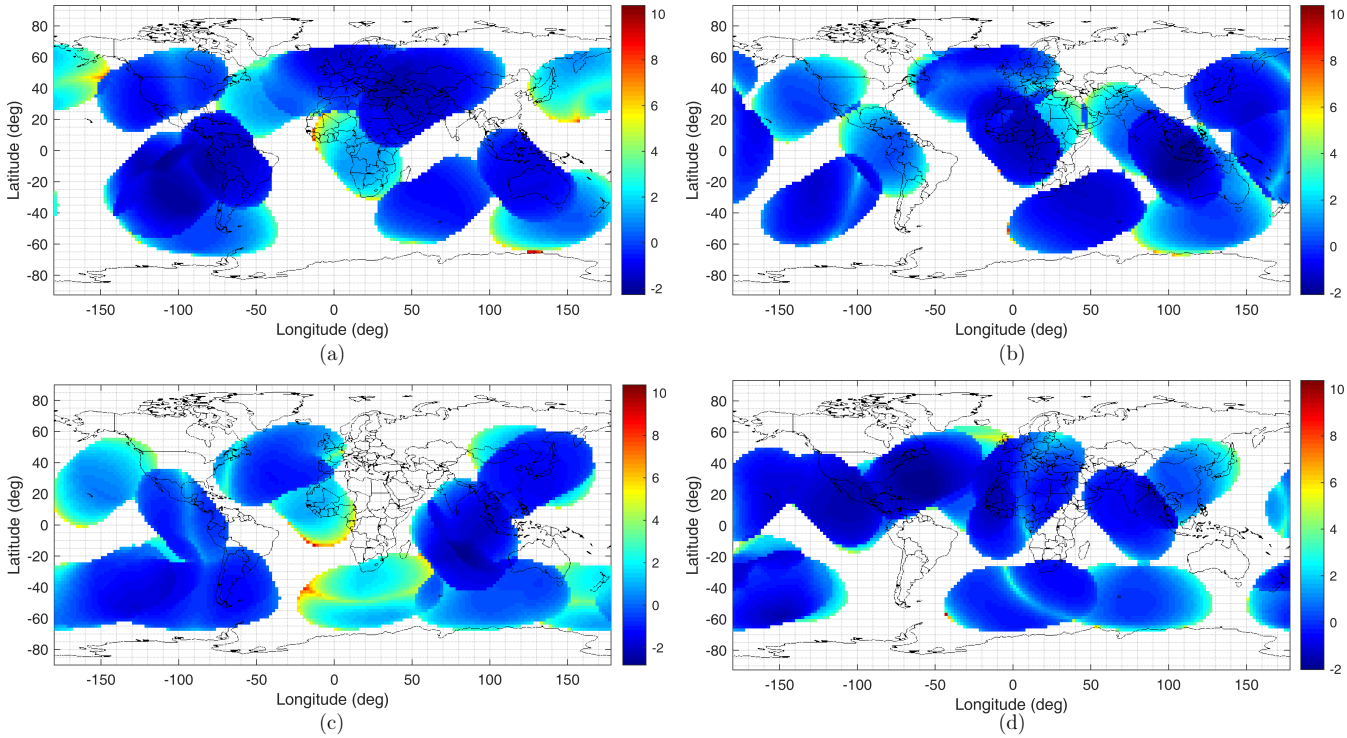

Fig. 4. Heat map of ln [PDOP] for the Orbcomm constellation and a wait time of 8 minutes. (a)–(d): The heat map is computed 4 times at 30 minute intervals, starting at midnight on June 27, 2019, UTC time.

B. Ionospheric and Tropospheric Delay Residuals

Next, the ionospheric and tropospheric delay residuals are studied as a function of the baseline, i.e., the distance between the base and the rover. The residual delays are significant in the case of Orbcomm LEO satellites since the obliquity factor changes significantly between different points on Earth, as illustrated in Figure 6. It was observed through simulations that a baseline of 2 km or less will keep the residual delays below 2 meters.

V. EXPERIMENTAL RESULTS

In this section, experimental results are presented demonstrating positioning with the CD-LEO framework developed in this paper. Only the 2–D position of the rover is estimated as its altitude may be obtained using other sensors (e.g., altimeter). In the following experiments, the altitude of the rover was obtained from its surveyed location.

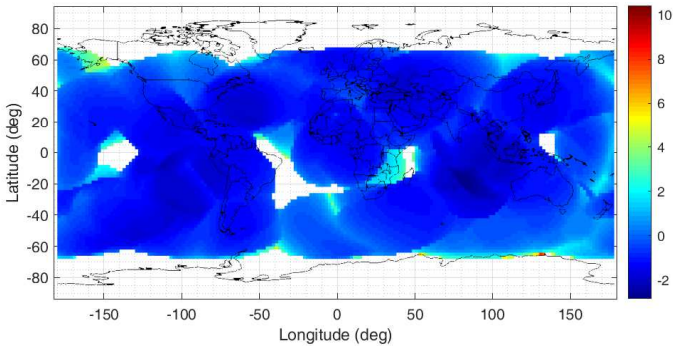

Fig. 5. Heat map of ln [PDOP] for the Orbcomm constellation and a wait time of 8 minutes combined over 2 hours.

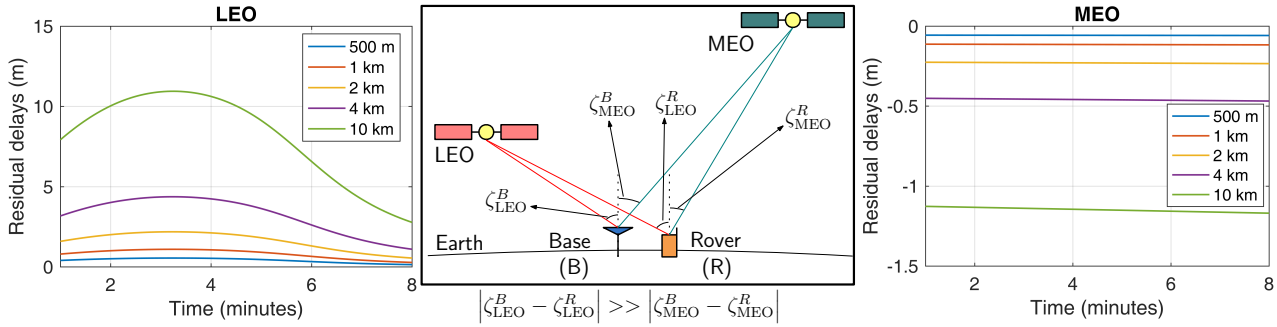

Fig. 6. Ionospheric delays observed by a terrestrial receiver for GPS and Orbcomm LEO satellites for varying baselines: 500 m, 1 km, 2 km, 4 km, and 8 km. The zenith angle ζ is defined as $\zeta \triangleq \pi/2 - \theta$, where θ is the elevation angle.

Moreover, the noise equivalent bandwidths of the receivers' PLLs were set to $B_{\rm R,PLL} = B_{\rm B,PLL} = B_{\rm PLL} = 18$ Hz. In order to demonstrate the CD-LEO framework discussed in Section III, the base, which was a DJI Matrice 600 UAV, was equipped with an Ettus E312 USRP, a high-end VHF antenna, and a small consumer-grade GPS antenna to discipline the on-board oscillator. The rover, which was a stationary receiver, was equipped with an Ettus E312 USRP, a custom-made VHF antenna, and a small consumer-grade GPS antenna to discipline the on-board oscillator. The receivers were tuned to a 137 MHz carrier frequency with more than 1 MHz sampling bandwidth, which covers the 137–138 MHz band allocated to Orbcomm SVs. Samples of the received signals were stored for off-line post-processing using a modified version of the software-defined radio (SDR) developed in [9]. The LEO carrier phase measurements were given at a rate of 4.8 kHz and were downsampled to 1 Hz. The ground-truth reference for the rover was surveyed on Google Earth, and the base UAV trajectory was taken from its on-board navigation system, which uses GNSS (GPS and GLONASS), an inertial measurement unit (IMU), and other sensors. The experimental setup is shown in Fig. 7.

The rover waited 114 s to produce a position estimate. Over the course of the experiment, the receivers on-board the base and the rover were listening to 2 Orbcomm SVs, namely FM 108 and FM 116, whose positions were decoded from the transmitted ephemeris and interpolated at 1 Hz rate. A sky plot of the 2 Orbcomm SVs is shown in Fig. 8(a). The Doppler frequency measured by the rover using the SDR in [9] for the 2 Orbcomm SVs is shown along the expected Doppler calculated from the TLE files in Fig. 8(b). The measured ionospheric and tropospheric delay residuals between the rover and base are shown with the estimated residual delays using the models in Subsection II-B are shown in Fig. 8(c). It can be seen that the estimated residual delays are negligible. The measured residual delays are mainly due to unmodeled errors. Note that the base was mobile during the experiment and the position returned by its on-board navigation system was used as ground-truth. Consequently, any errors in the UAV's navigation solution would have reflected in the residual delays and degraded the rover's position estimate.

The CD-LEO measurements were used to estimate the rover's position via the base/rover framework developed in Section III. The SVs' trajectories, the true and estimated rover position, as well as the base UAV trajectory are shown in Fig. 9. The position error was found to be 11.93 m. The PDOP was found to be 29.17. Assuming a precision of $\lambda/2$ in the CD-LEO measurements, it is found that the position error obtained in this experiment is well below the $1-\sigma$ bound.

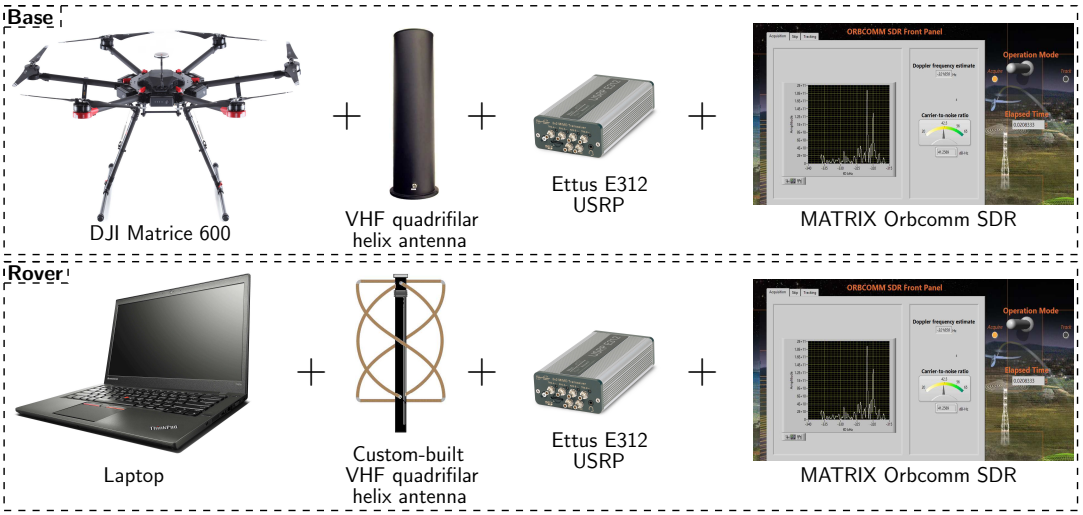

Fig. 7. Base/rover experimental setup of the CD-LEO framework.

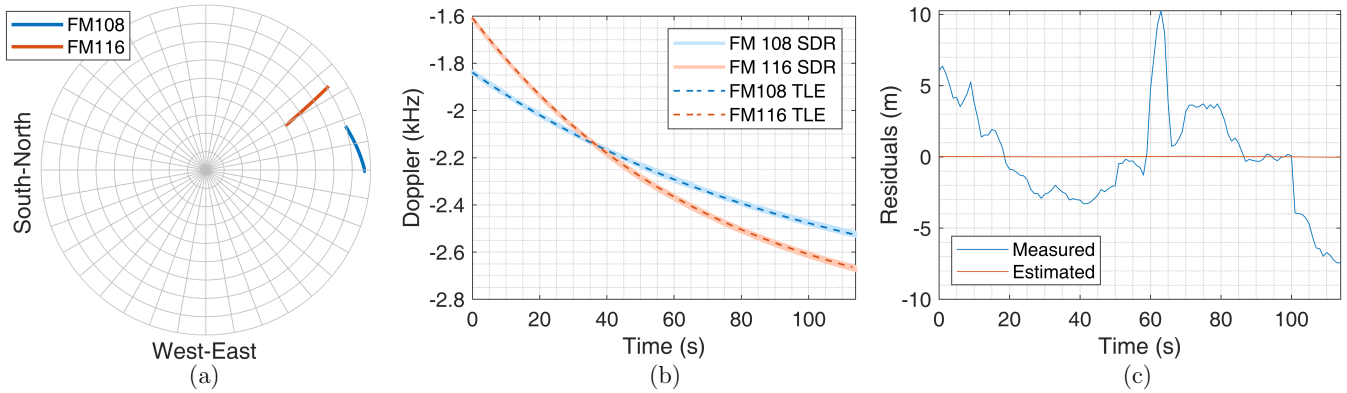

Fig. 8. (a) Sky plot showing the geometry of the 2 Orbcomm SVs during the experiment. (b) The measured Doppler frequencies using the proprietary SDR and the expected Doppler calculated from the TLE for both Orbcomm SVs. (c) Measured and estimated ionospheric and tropospheric residual delays.

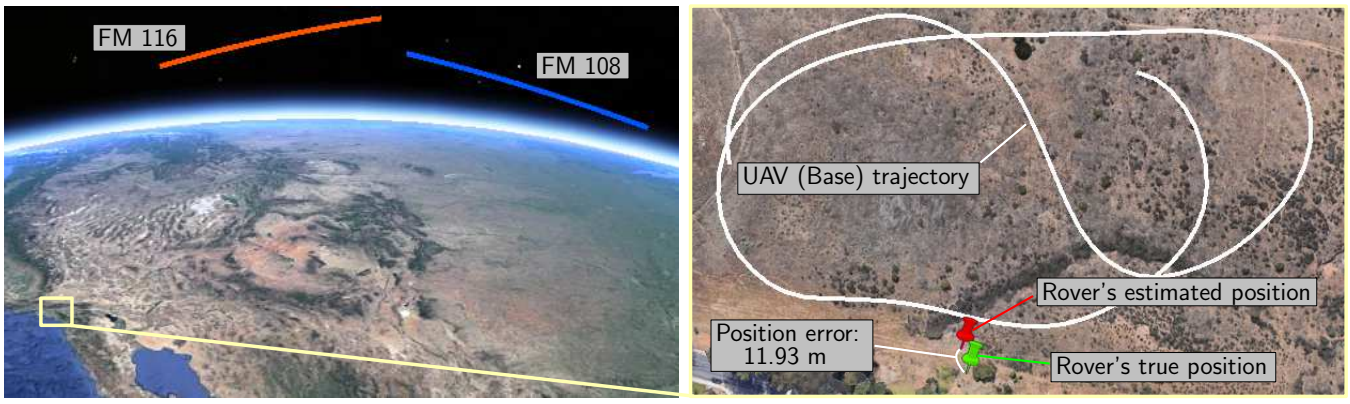

Fig. 9. Trajectory of the 2 Orbcomm SVs during the experiment, trajectory of the base UAV, and the rover's true and estimated position. Map data: Google Earth.

VI. CONCLUSION

This paper proposed a framework for positioning with CD-LEO measurements. The base/rover framework focuses on the Orbcomm constellation and does not require prior knowledge of the rover's position. The effect of ionospheric and tropospheric delays on the carrier phase and CD-LEO measurements were discussed. The residual ionospheric

and tropospheric delays were studied as a function of the baseline, and it was found that a baseline of 2 km or less keeps the residual delays negligible. Moreover, the PDOP was studied for the Orbcomm constellation, and it was found that a less than unity PDOP may be achieved for 8-minute wait times. An experiment was conducted showing a receiver positioning itself exclusively with CD-LEO measurements from 2 Orbcomm SVs with a position error of 11.93 m.

Acknowledgment

This work was supported in part by the Office of Naval Research (ONR) under Grant N00014-16-1-2305 and Grant N00014-19-1-2511 and in part by the National Science Foundation (NSF) under Grant 1929965. The authors would like to thank Joshua Morales, Linh Nguyen, Ali Abdallah, Mohammad Orabi, Kimia Shamaei, Mahdi Maaref, and Naji Tarabay for their help in data collection.

References

[1] M. Joerger, L. Gratton, B. Pervan, and C. Cohen, "Analysis of Iridium-augmented GPS for floating carrier phase positioning," *NAVIGATION, Journal of the Institute of Navigation*, vol. 57, no. 2, pp. 137–160, 2010.

[2] K. Pesyna, Z. Kassas, and T. Humphreys, "Constructing a continuous phase time history from TDMA signals for opportunistic navigation," in *Proceedings of IEEE/ION Position Location and Navigation Symposium*, April 2012, pp. 1209–1220.

[3] T. Reid, A. Neish, T. Walter, and P. Enge, "Broadband LEO constellations for navigation," *NAVIGATION, Journal of the Institute of Navigation*, vol. 65, no. 2, pp. 205–220, 2018.

[4] J. Morales, J. Khalife, A. Abdallah, C. Ardito, and Z. Kassas, "Inertial navigation system aiding with Orbcomm LEO satellite Doppler measurements," in *Proceedings of ION GNSS Conference*, September 2018, pp. 2718–2725.

[5] Z. Kassas, J. Morales, and J. Khalife, "New-age satellitebased navigation – STAN: simultaneous tracking and navigation with LEO satellite signals," *Inside GNSS Magazine*, vol. 14, no. 4, pp. 56–65, 2019.

[6] J. Morales, J. Khalife, U. S. Cruz, and Z. Kassas, "Orbit modeling for simultaneous tracking and navigation using LEO satellite signals," in *Proceedings of ION GNSS Conference*, September 2019.

[7] T. Reid, A. Neish, T. Walter, and P. Enge, "Leveraging commercial broadband LEO constellations for navigating," in *Proceedings of ION GNSS Conference*, September 2016, pp. 2300–2314.

[8] J. Morales, J. Khalife, and Z. Kassas, "Simultaneous tracking of Orbcomm LEO satellites and inertial navigation system aiding using Doppler measurements," in *Proceedings of IEEE Vehicular Technology Conference*, April 2019, pp. 1–6.

[9] J. Khalife and Z. Kassas, "Receiver design for Doppler positioning with LEO satellites," in *Proceedings of IEEE International Conference on Acoustics, Speech and Signal Processing*, May 2019, pp. 5506–5510.

[10] C. Ardito, J. Morales, J. Khalife, A. Abdallah, and Z. Kassas, "Performance evaluation of navigation using LEO satellite signals with periodically transmitted satellite positions," in *Proceedings of ION International Technical Meeting Conference*, 2019, accepted.

[11] Z. Kassas, "Collaborative opportunistic navigation," *IEEE Aerospace and Electronic Systems Magazine*, vol. 28, no. 6, pp. 38–41, 2013.

[12] J. McEllroy, "Navigation using signals of opportunity in the AM transmission band," Master's thesis, Air Force Institute of Technology, Wright-Patterson Air Force Base, Ohio, USA, 2006.

[13] S. Fang, J. Chen, H. Huang, and T. Lin, "Is FM a RF-based positioning solution in a metropolitan-scale environment? A probabilistic approach with radio measurements analysis," *IEEE Transactions on Broadcasting*, vol. 55, no. 3, pp. 577–588, September 2009.

[14] R. Faragher and R. Harle, "Towards an efficient, intelligent, opportunistic smartphone indoor positioning system," *NAVIGATION, Journal of the Institute of Navigation*, vol. 62, no. 1, pp. 55–72, 2015.

[15] J. Khalife, Z. Kassas, and S. Saab, "Indoor localization based on floor plans and power maps: Non-line of sight to virtual line of sight," in *Proceedings of ION GNSS Conference*, September 2015, pp. 2291–2300.

[16] W. Xu, M. Huang, C. Zhu, and A. Dammann, "Maximum likelihood TOA and OTDOA estimation with first arriving path detection for 3GPP LTE system," *Transactions on Emerging Telecommunications Technologies*, vol. 27, no. 3, pp. 339–356, 2016.

[17] A. Tahat, G. Kaddoum, S. Yousefi, S. Valaee, and F. Gagnon, "A look at the recent wireless positioning techniques with a focus on algorithms for moving receivers," *IEEE Access*, vol. 4, pp. 6652–6680, 2016.

[18] K. Shamaei, J. Khalife, and Z. Kassas, "Exploiting LTE signals for navigation: Theory to implementation," *IEEE Transactions on Wireless Communications*, vol. 17, no. 4, pp. 2173–2189, April 2018.

[19] J. Khalife and Z. Kassas, "Navigation with cellular CDMA signals – part II: Performance analysis and experimental results," *IEEE Transactions on Signal Processing*, vol. 66, no. 8, pp. 2204–2218, April 2018.

[20] Z. Kassas, J. Khalife, K. Shamaei, and J. Morales, "I hear, therefore I know where I am: Compensating for GNSS limitations with cellular signals," *IEEE Signal Processing Magazine*, pp. 111–124, September 2017.

[21] J. Khalife and Z. Kassas, "Precise UAV navigation with cellular carrier phase measurements," in *Proceedings of IEEE/ION Position, Location, and Navigation Symposium*, April 2018, pp. 978–989.

[22] J. Khalife, K. Shamaei, S. Bhattacharya, and Z. Kassas, "Centimeter-accurate UAV navigation with cellular signals," in *Proceedings of ION GNSS Conference*, September 2018, pp. 2321–2331.

[23] D. Lawrence, H. Cobb, G. Gutt, M. OConnor, T. Reid, T. Walter, and D. Whelan, "Navigation from LEO: Current capability and future promise," *GPS World Magazine*, vol. 28, no. 7, pp. 42–48, July 2017.

[24] P. Misra and P. Enge, *Global Positioning System: Signals, Measurements, and Performance*, 2nd ed. Ganga-Jamuna Press, 2010.

[25] Ionospheric and atmospheric remote sensing. Accessed October 1, 2019. [Online]. Available: https://iono.jpl.nasa.gov/